RSC Advances

ROYAL SOCIETY OF CHEMISTRY

www.rsc.org/advances

Cite this: DOI: 10.1039/c0xx00000

ARTICLE

Two Schiff base ligands for distiguishing Zn^{II}/Cd^{II} sensing — effect of substituent on fluorecent sensing †

Zhi-Peng Zheng,[a] Qin Wei,[a] Wen-Xia Yin,[a] Lin-Tao Wan,[a] Xia Huang[a], Ying Yu*[a], Yue-Peng Cai*,[a,b]

Received (in XXX, XXX) Xth XXXXXXXXX 20XX, Accepted Xth XXXXXXXXX 20XX
DOI: 10.1039/b000000x

Two Schiff base ligands (**HL^1, HL^2**) were conveniently synthesised by one-step condensation between pyridine 2-ylmethanamine and 3-ethoxy-2-hydroxybenzenaldhyde (for **HL^1**) or salicylaldehyde (for **HL^2**) as fluorescent sensors for distinguishing sensing of Zn^{2+}or Cd^{2+}. Both of the two fluorescent sensors present very weak emission at 463 nm (for **HL^1**) or 453 nm (for **HL^2**). For **HL^1**, upon addition of Zn^{2+}, fluorescence intensity of **HL^1** enhanced and gradually red shifted to 493 nm with a green emission while addition of Cd^{2+} only induced enhancement of fluorescent intensity at 463 nm. For **HL^2**, only addition of Zn^{2+} induced enhancement of fluorescence intensity, presenting a high Zn^{2+}/Cd^{2+} selectivity. Zn^{2+}-induced red shift in fluorescent spectra of **HL^1** could be attributed to the twisted intramolecular charge transfer (TICT) from the interaction between Zn^{2+} ion and in situ formed ligand **$L^{1'}$** with the twisted structure in compound **1**, which is absent in compound **2**. The Zn^{2+}/Cd^{2+} selectivity of fluorescent response for **HL^2** correlates with the Cd-**HL^2** and Zn-**HL^2** coordination bond distances. Obviously, introduction of ethoxyl groups onto benzene ring as an electron-donating group facilitates the Zn-induced in situ dimerization of **HL^1** into new ligand **$L^{1'}$** with twisted molecular structure, further resulting in red shift of fluorescent spectra.

Introduction

Fluorescent sensor for metal ions is one of the most sought-for detection methods for metal ions owing to its convenient use, high selectivity, potential use in living cells and discernible response with color variation under UV irradiation or with naked eye.[1] Whether in protein-bound or free form, Zn^{2+} is a type of abundant ion among the trace metal ions in human's body and is greatly related to many crucial biological processes including nervous system's function, enzyme regulation, gene expression, biological catalysis and Zn(II)-disorder-related diseases.[2] Zn^{2+} is also environmentally important because increased level of Zn^{2+} inwater can cause environmental problems including poor soil microbial activity causing phytotoxic effects or smelly water.[3] Amount of fluorescent sensors have been developed to investigate the distribution of mobile Zn^{2+} in living cells over the last decades which are mainly based on metal complexation and complexation-based photoinduced electron-transfer (PET), chelation-enhanced-fluorescence (CHEF) effect or internal charge-transfer (ICT) mechanism.[4] Twisted intramolecular charge transfer (TICT) based on twisted molecular structure is among the types of ICT and is widely employed in fluorescent ion sensing due to its spectral shifts and color variation originating from locally emission (LE) band and TICT emission band.[1c,5] Theoretically, introduction of electron donating groups (e.g. –OR, –R) and electron withdrawing groups (e.g. $–NO_2$, –CN) onto the moiety of the organic sensor, may generate TICT upon coordination of the ligand with metal ions, based on which metal ions sensing could be achieved.[5,6] On the other hand, the detection of Zn^{2+} is often related to Cd^{2+} because of their similar electron configurations and similar response to the same fluorescent sensor, making one of the biggest challenges in constructing Zn^{2+} fluorescent chemosensor.[7] Moreover, because of cadmium's accumulation in the food chain and its great toxicity to human's body,[8] it is desirable to develop some analytical methods for cadmium detection in the environment or living cells. Therefore, it is necessary to develop fluorescent sensor for distinguishing sensing of Zn^{2+} and Cd^{2+}.

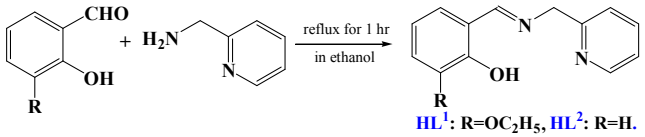

HL^1: R=OC_2H_5, HL^2: R=H.

Scheme 1. Synthesis of **HL^1** and **HL^2**.

Based on the above considerations, we designed and synthesized two Schiff base ligands **HL^1** and **HL^2** for distinguishing sensing of Zn^{2+} and Cd^{2+}. Ethoxyl group as electron donating group was introduced onto **HL^1** endowing it with TICT property and subsequent spectral shift upon reaction with Zn^{2+}. **HL^1** and **HL^2**

[a] *School of Chemistry and Environment, South China Normal University; Guangzhou Key Laboratory of Materials for Energy Conversion and Storage, Guangzhou 510006, P.R. China. Fax: +86-020-39310; Tel: +86-020-39310383; E-mail: caiyp@scnu.edu.cn*
[b] *State Key Laboratory of Structure Chemistry, Fujian, Fuzhou 350002, PR China*

*† Electronic Supplementary Information (ESI) available. CCDC 1003835, 1003836, 1003837, 1003838 are for compounds **1-4**, respectively. For ESI and crystallographic data in CIF or other electronic format see DOI: 10.1039/b000000x/*

were conveniently obtained through one-step condensation (scheme **1**) between pyridine 2-ylmethanamine and 3-ethoxy-2-hydroxybenzenaldhyde (for **HL^1**) or salicylaldehyde (for **HL^2**). Compared with other previously reported Zn^{2+} organic sensor[4], **HL^1** and **HL^2** present distinct advantages including its convenient synthesis and tridentate donor set of N_2O capable of strongly chelating to Zn^{2+} or Cd^{2+} ions through forming five/six membered ring with common side, providing a binding site between metal ions and sensor. For **HL^2**, together with the pyridine ring as electron withdrawing group[9], introduction of ethoxyl group as electron donating group onto the benzene ring facilitates the internal charge transfer of the sensor and further presents Zn-induced TICT and spectral red shift, which does not exist in the system of **HL^2** owing to absence of ethoxyl group. However, without ethoxyl group as hindrance effect, **HL^2** shows greater sensitivity towards sensing Zn^{2+} with a much lower detection limit.

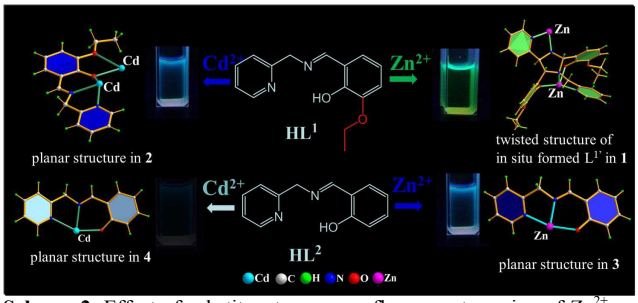

Scheme 2. Effect of substituent group on fluorescent sensing of Zn^{2+} and Cd^{2+} based on Schiff base complexes **1**-**4**.

Experimental

General procedures. All chemicals were of analytical reagent grade and were used as received without any further purification. Elemental analysis for C, H, and N were performed on a Perkin-Elmer 2400 analyzer. IR spectra were recorded with a Perkin-Elmer Fourier transform infrared spectrophotometer with samples prepared as KBr disks in the 4000−400 cm^{-1} range. UV-vis absorption spectra were recorded on a shimadzu UV1800 UV-vis Spectrophotometer. Fluorescent spectra were recorded on a Hitachi F-2500 spectrometer with the excitation slit as 5 nm and emission slit as 5 nm.

X-ray Crystallography Crystal data collections were performed at 298 K on a Bruker Smart Apex II diffractometer with graphitemono-chromated Mo Kα radiation (λ = 0.71073 Å) for four compounds **1**−**4**. Absorption corrections were applied by using the multi-scan program SADABS[10]. Structural solutions and full-matrix least-squares refinements based on F^2 were performed with the SHELXS-97[11] and SHELXL-97[12] program packages, respectively. All the non-hydrogen atoms were refined anisotropically. The hydrogen atoms on organic motifs were placed at calculated positions. Details of the crystal parameters, data collections, and refinements for compounds **1**−**4** are summarized in Table **S1**. Selected bond lengths and angles of compounds **1**−**4** are shown in Table **S2**. CCDC 1015499-1015501, 1015694 are for the four new compounds **1**−**4,** respectively. These data can be obtained free of charge from The Cambridge Crystallographic Data Centre via www.ccdc.cam.ac.uk/data request/cif.

Synthesis of HL^1 and HL^2.

The Schiff-base ligand 2-ethoxy-6((pyridin-2-ylmethylimino)-methyl)phenol (**HL^1**) was synthesized according to corresponding reference [13].2-((pyridin-2-ylmethylimino)methyl)-phenol (**HL^2**) was prepared according to related reference[14].

Synthesis of Compounds 1-4.

$[Zn_4(L^1)(L^{1'})Cl_5]$ (1). After refluxing at 60°C for 1 hour, to a mixed solution of 3-ethoxy-2-hydroxybenzenaldhyde (0.2 mmol, 33.2 mg) and 2-pyridin-2-ylmethanamine (0.2 mmol 21μL) in MeOH (20 mL) was added $ZnCl_2$ (0.2 mmol, 27 mg). The resulting clear yellow solution was stirred for 1 more hour at room temperature and then filtered. After 2 weeks, pale yellow needle-shaped crystals of compound $[Zn_4(L^1)(L^{1'})Cl_5]$ (**1**) was obtained after slow diffusion of petroleum ether into the resulted clear solution. Yield (based on $ZnCl_2$): 45mg (75%). IR (KBr cm^{-1}):3417(br, vs), 2980(w), 2894(w), 1631(s), 1604(m), 1556(m), 1487(m), 1460(m), 1427(w), 1388(m), 1273(m), 1246(w), 1217(s), 1110(w), 1047(s), 991(w), 904(w), 842(w), 783(s), 738(m), 663(m), 561(s), 468(m). Elemental analysis calcd (%) for $C_{45}H_{44}Cl_5N_6O_6Zn_4$: C, 44.90; H, 3.68; N, 6.98; Found: C, 44.70; H, 3.69; N, 7.01.

$[Cd_2(L^1)Cl_2(DMSO)]_2$ (2). The procedure was the same as that for **1** using $CdCl_2{\cdot}2.5H_2O$ (0.2mmol 46mg) instead of $ZnCl_2$, and drops of DMSO were added to dissolve the resulting precipitate after stirring. After 1 week, pale yellow needle-shaped crystals of $[Cd_2(L^1)Cl_2(DMSO)]_2$ (**2**) were obtained after slow diffusion of petroleum ether into the resulted clear solution. Yield (based on $CdCl_2$): 29.6 mg(60%). IR (KBr cm^{-1}): 3478 (br, vs), 3304 (w), 2970(w), 1635(vs), 1558(vs), 1420(m), 1413(s), 1303(w), 1280(w), 1234(w), 1209(s), 1151(w), 1078(m), 1041(m), 906(w), 767(m), 746(m), 642(m), 524(w), 443(w). Elemental analysis calcd (%) for $C_{34}H_{42}Cd_4Cl_6N_4O_6S_2$: C, 30.72; H, 3.18; N, 4.22; Found: C, 30.80; H, 3.13; N, 4.26.

$[Zn(L^2)Cl]_2$ (3). The procedure was the same as that for **1** using salicylaldehyde (21μL, 0.2 mmol) instead of 3-ethoxy-2-hydroxybenzenaldhyde. Pale yellow single crystals of **3** were formed in three days. Yield (based on $ZnCl_2$): 51.1mg (82 %). IR (KBr cm^{-1}): 3439(s), 1637(s), 1595(w), 1552(m), 1469(s), 1413(m), 1350(w), 1290(s), 1197(w), 1145(w), 1064(w), 1001(w), 906(w), 837(w), 761(s), 661(w), 582(w), 439(w). Elemental analysis calcd (%) for $C_{26}H_{22}Cl_2N_4O_2Zn_2$: C, 50.03; H, 3.55; N, 8.98; Found: C, 50.18; H, 3.59; N, 9.13.

$\{[Cd_4L^2_6]^{2+}{\cdot}[CdCl_4]^{2-}{\cdot}CH_3OH\}_2{\cdot}H_2O$ (4). The procedure was the same as that for **2** using salicylaldehyde (21 μL, 0.2 mmol) instead of 3-ethoxy-2-hydroxybenzenaldhyde. Pale yellow single crystals of **4** were formed in two weeks. Yield (based on $CdCl_2$): 35.2mg (44%). IR (KBr cm^{-1}): 3443(s), 2980(m), 1634(s), 1598(w), 1562(m), 1467(s), 1403(m), 1355(w), 1290(s), 1199(w), 1155(w), 1074(w), 1081(w), 918(w), 844(w), 766(s), 677(w), 562(w), 449(w). Elemental analysis calcd (%) for $C_{158}H_{142}Cd_{10}Cl_8\ N_{24}O_{15}$: C, 47.15; H, 3.56; N, 8.35; Found: C, 47.14; H, 3.57; N, 8.34.

Results and discussion

Fluorescence/UV absorption Spectra and Titration of HL^1.

The fluorescence response of receptor **HL^1** towards Zn^{2+} was studied in 0.10 mM ethanol. Upon excitation at 350 nm, **HL^1** in ethanol presented dark blue emission at 463 nm which could be attributed to the intraligand π-π* transition[15]. With stepwise addition of $ZnCl_2$ solution in ethanol with concentration ranging

from 0.1 equiv to 2.0 equiv., fluorescent emission of **HL^1** gradually red-shifted to 493 nm with their fluorescent intensity at 493nm enhanced linearly with the Zn^{2+} concentration and saturated when [Zn^{2+}] reaches 1.33 equiv. (Figure **1**). Interaction between Zn^{2+} and **HL^1** was also studied by UV absorption spectra (Figure **S1**). Concomitant addition of $ZnCl_2$ into **HL^1** in ethanol causes a new absorption peak at 380nm with intensity increased while that at 220nm, 264nm, 334, 432 nm decreased with four isosbetic points at 249, 276, 303, 347 nm. The binding ratio between Zn^{2+} and ligand was estimated to be 4:3 as confirmed by its job plot (Figure **S2**) and crystal structure. The limit of detection (LOD) was measured to be 1.11×10^{-6} M (R^2= 0.999) with a linearity range between 1×10^{-5}M and 9×10^{-5}M (LOD = 3σ/slope) (Figure **S3**).

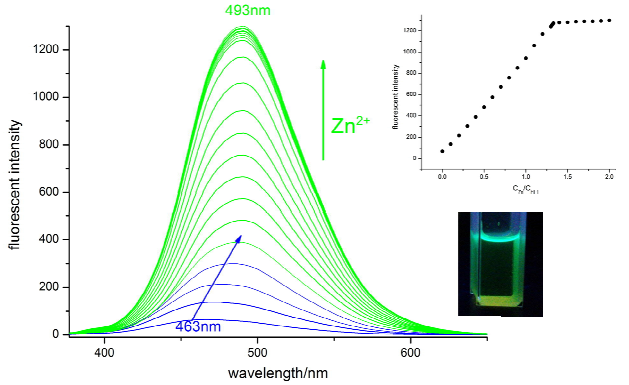

Figure 1. Fluorescence emission spectra of **HL^1** upon addition of $ZnCl_2$ in ethanol. λ_{ex} = 350 nm at room temperature ([**HL^1**] =0.10 mM; [Zn^{2+}] =0, 0.01, 0.02, 0.03, 0.04, 0.05, 0.06, 0.07, 0.08, 0.09, 0.10, 0.11, 0.12, 0.13,0.131, 0.132,0.133, 0.14, 0.15, 0.16, 0.17, 0.18, 0.19, 0.20 mM. (Inset: Corresponding $ZnCl_2$ titration profile according to the fluorescence intensity, indicating 4:3 stoichiometry for Zn^{2+}/**HL^1**.)

The selectivity of **HL^1** to Zn^{2+} was examined by fluorescence titration of **HL^1** with various metal ions (Figure **2**). The fluorescence intensity of **HL^1** was slightly quenched with some cations such as Ni^{2+}, Cu^{2+}, Co^{2+}, and Fe^{3+}, Mn^{2+}. Other cations such as Na^+, K^+, Li^+, Mg^{2+}, Ba^{2+}, Ca^{2+}, Hg^{2+}, Fe^{2+}, Pb^{2+}, Al^{3+} and Cr^{3+} did not cause any significant changes, showing selective CHEF & spectral red shift in the presence of Zn^{2+}. Nevertheless, interaction of Cd^{2+} with **HL^1** also presents fluorescence spectral response which is relatively weaker compared with that of Zn^{2+}. Concomitant addition of $CdCl_2$ into **HL^1** in ethanol induced enhancement of the ligand-centered emission (Figure **3**) with binding ratio between Cd^{2+} and **HL^1** as 2:1 confirmed by job plot (Figure **S4**) and crystallography with a limit of detection as 9.2×10^{-6}M (R^2= 0.999) with a linearity range between 2×10^{-5} to 1.8×10^{-4} M (LOD = 3σ/slope) (Figure **S5**). UV absorption

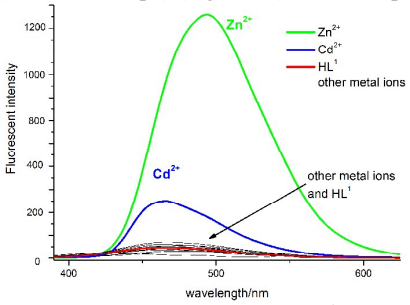

Figure 2. Fluorescence emission spectra of **HL^1** in the presence of different ions such as Na^+, K^+, Mg^{2+}, Ca^{2+}, Cu^{2+}, Co^{2+}, Al^{3+}, Cr^{3+},Ni^{2+}, Fe^{2+}, Fe^{3+}, Zn^{2+}, Cd^{2+}, Mn^{2+}, Hg^{2+}, and Pb^{2+} (metal ions as their Cl^- and Hg^{2+},Pb^{2+} as their NO_3^-salts) in ethanol. λ_{ex} = 350 nm, [**HL^1**] = 0.1 mM, and [M^{n+}] = 0.2 mM.

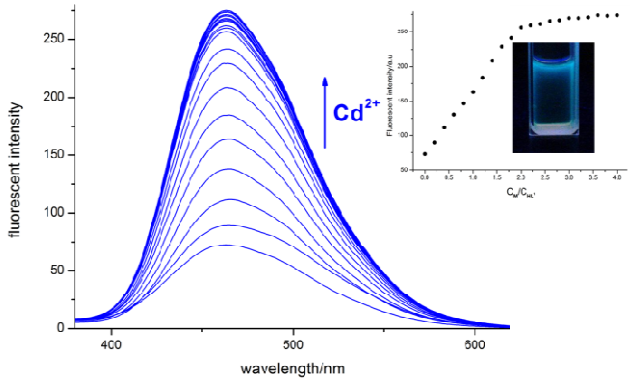

Figure 3. Fluorescence emission spectra of **HL^1** upon addition of $CdCl_2$ in ethanol. λ_{ex} = 350 nm at room temperature ([**HL^1**] =0.10 mM; [Cd^{2+}] =0, 0.02, 0.04, 0.06, 0.08, 0.1, 0.12, 0.14, 0.16, 0.18, 0.20, 0.22, 0.24, 0.26, 0.28, 0.30, 0.32, 0.34, 0.36, 0.38, 0.40 mM. (Inset: Corresponding $CdCl_2$ titration profile according to the fluorescence intensity, indicating 2:1 stoichiometry for Cd^{2+}/**HL^1**.)

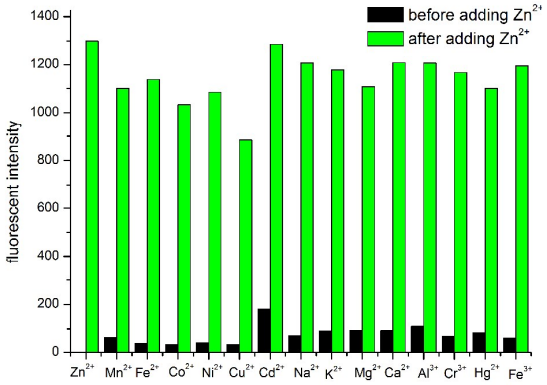

Figure 4. Selectivity of **HL^1** for Zn^{2+} in the presence of other metal ions in ethanol. λ_{ex} = 350 nm. Black bars represent the addition of an excess of the appropriate metal ion (0.5 mM for Na^+, K^+, Ca^{2+}, Mg^{2+}, Fe^{3+}, and Cu^{2+} and 0.3 mM for all other metal ions) to a 0.1M solution of **HL^1**. Green bars represent the subsequent addition of 0.1 mM $ZnCl_2$ to the solution.

titration also demonstrates interaction between Cd^{2+} and **HL^1** (Figure **S6**). The selectivity of **HL^1** on Zn^{2+} over Cd^{2+} was determined as 4.8 calculated from ratio of I_{Zn}/I_{Cd} (2 equiv.).

To further evaluate selectivity of **HL^1** towards Zn^{2+}, the interference of series of metal ions on detection of Zn^{2+} was examined. Seeing from Figure **4**, in the presence of various metal ions including Na^+, K^+, Ca^{2+}, Mg^{2+}, Fe^{3+}, Hg^{2+}, Mg^{2+} and Cd^{2+}, the emission intensity of **HL^1**-Zn remain hardly perturbed, while in the vicinity of other involved metals, it is slightly quenched but is still clearly detectable, indicating a high selectivity of **HL^1** on Zn^{2+}.

Crystal structure of $Zn_4L^1L^{1'}Cl_5$ (1) and $[Cd_2(L^1)Cl_2$-(DMSO)]$_2$ (2) and proposed mechanism of HL^1 sensing Zn^{2+}/Cd^{2+}

Reaction of **HL^1** with Zn^{2+} induced part of **HL^1** to undergo [3+2] cycloaddition[16] generating a dimerized form of **L$^{1'}$** (Scheme **S1**) and compound **1** was formed. Crystal analysis revealed thatcompound **1** crystallized in triclinic *P*-1 space group and each discrete tetranuclear unit comprised of four Zn^{2+} ions, one dimerized ligand **L$^{1'}$**, one original Schiff base ligand **L^1** and five chlorides. As shown in Figure **5**, out of the four Zn ions, Zn1 was penta-coordinated to one pyridine nitrogen atom (N2), one amide nitrogen (N4), two hydroxyl oxygen atoms (O3, O4) all from **L$^{1'}$**, while Zn2 was four-coordinated to one hydroxyl oxygen atom of

$L^{1'}$and three chlorides (one μ_2-bridged Cl2 and the other two terminal coordinated Cl1, Cl5). And Zn3 was penta-coordinated to one hydroxyl oxygen atom (O3) of $\mathbf{L^{1'}}$, two N atoms (N1, N2), one O atom (O1) of $\mathbf{L^1}$ and one μ_2-bridged chlorides (Cl2), connecting L^1 and $L^{1'}$ together while Zn4 was quadra-coordinated to two nitrogen atoms (N5 N6) from $\mathbf{L^{1'}}$ and two terminal chlorides (Cl3, Cl4). Moreover, π···π stacking between benzene ring and pyridine ring helps to stabilize structure of compound **1**(Figure **5b)**

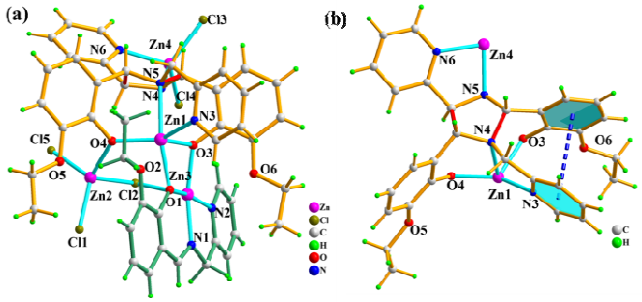

Figure 5. a) Molecular structure of compound $Zn_4(\mathbf{L^1})(\mathbf{L^{1'}})Cl_5$ (**1**) with partial atomic labels and b) twisted conformation of the dimerized form of $\mathbf{L^{1'}}$ accounting for the TICT and spectral red-shift.

When reacted with $CdCl_2$, $\mathbf{HL^1}$ generated compound $[Cd_2(\mathbf{L^1})Cl_2(DMSO)]_2$ (**2**), which crystallized in triclinic, *P*-1 space group presenting a centrosymmetric discrete tetra-nuclear structure (Figure **6**). Its asymmetric unit contained two Cd^{2+} ions, one depotonated $(\mathbf{L^1})^-$ anion, three chlorides and one coordinated DMSO molecule. Cd1 was penta-coordinated to one pyridine nitrogen atom (N1), one azomethine amide nitrogen atom (N2), one hydroxyl oxygen atom (O1) and two chlorides (Cl1, Cl1, one

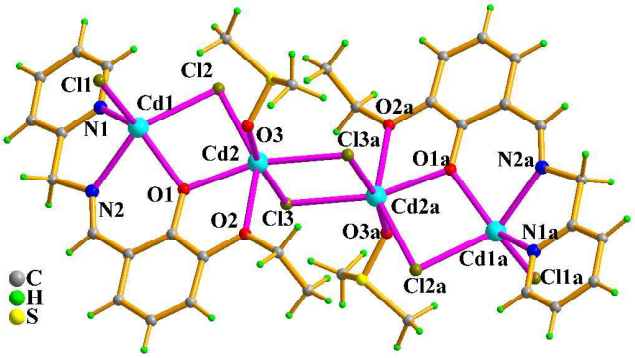

Figure 6. Molecular structure of tetranuclear compound $[Cd_2(\mathbf{L^1})Cl_2$-$(DMSO)]_2$ (**2**) with partial atomic labels. Asymmetry code: a)1-x,2-y,1-z.

μ_2-bridged and the other terminal coordinated), exhibiting a distorted square pyramid coordination geometry. The other Cd2 ion is hexa-coordinated with two μ_2-bridged chlorides (Cl2, Cl3), one hydroxyl oxygen atom (O1), one ethoxyl oxygen atom (O2) and one oxygen atom (O3) from the DMSO molecule, showing distorted octahedral coordination geometry. Moreover, by μ_2-bridging of two chlorides (Cl3, Cl3a), two asymmetric units were connected to assemble a tetranuclear unit of compound **2**.

Emission spectra of compounds **1**-**2** in ethanol also accord with emission spectra generated from titration, further confirming that the products formed upon titration are compounds **1** and **2** (Figure **S7**). Hence, mechanism for Cd^{2+} and Zn^{2+} sensing of $\mathbf{HL^1}$ could be proposed referring to the structural analysis of compound **1** and **2**. Compound **1** was obtained through reaction of $ZnCl_2$ with $\mathbf{HL^1}$, in which $\mathbf{HL^1}$ as 1, 3-dipole undergoes Zn-induced dimerization through [3+2] cycloaddition, generating a five-membered ring between two mole of $\mathbf{HL^1}$ (Scheme **S1**). Viewing from the top of the five-membered ring, it is not difficult to find that $\mathbf{L^{1'}}$ was fixed to present a twisted molecular structure, in which the pyridine ring and benzene ring was almost twisted to be orthogonal. Such twisted structure induced a twisted-intramolecular charge transfer state upon excitation which narrowed down the energy gap between HOMO and LUMO, generating an emission peak of longer wavelength at 493nm (Figure **7**).[5a, 17] Unlike compound **1**, in compound **2**, coordinated $\mathbf{L^1}$ presents a planar structure with the angle between the pyridine ring and benzene ring as nearly 0° (Figure **7**). Therefore, reaction of Cd^{2+} with $\mathbf{HL^1}$ presented locally excited (LE) emission at 463nm.

Furthermore, fluorescent intensity enhancement of $\mathbf{HL^1}$ upon interaction with Zn^{2+} or Cd^{2+} should be ascribed to the CHFF (chelation enhanced fluorescence), inhabitation of C=N isomerization[9,18] and weaken of PET[9] (photo induced charge transfer) process in the ligand. On the other hand, different coordination structure of compounds **1** and **2** are probably related to the difference in radius between Cd^{2+} (0.96 Å) and Zn^{2+} (0.74 Å), which also affects the extend of the CHEF effect on the chromphores. Moreover, the greater heavy atom quenching effect of Cd^{2+} also conduces to weaker spectral response of $\mathbf{HL^1}$ on Cd^{2+} than that of Zn^{2+}.

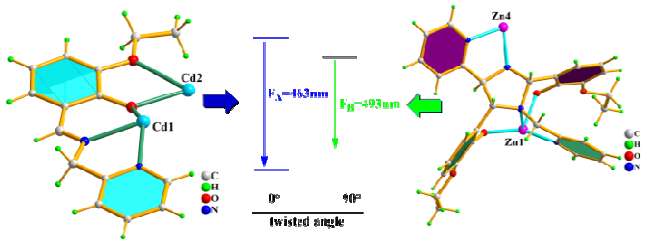

Figure 7. Diagram presenting planar structure of ligand $\mathbf{L^1}$ in compound **2** and twisted structure of $\mathbf{L^{1'}}$ in compound **1** accounting for locally excited (LE) emission at 463 nm and TICT emission at 493 nm, respectively.

Fluorescence/UV absorption Spectra and Titration of $\mathbf{HL^2}$.

Twisted molecular structure of compound **1** could be ascribed to introduction of ethoxyl group which facilitates internal charge transfer of $\mathbf{HL^1}$. In order to explore the effect of ethoxyl group on its spectral response to Zn^{2+} and Cd^{2+}, we choose $\mathbf{HL^2}$ absent of an ethoxyl group (Scheme **1**) to examine its spectral response towards Zn^{2+}/Cd^{2+} and found that $\mathbf{HL^2}$ has high selectivity on Zn^{2+} sensing with much more sensitivity.

The fluorescent spectral response of $\mathbf{HL^2}$ toward Zn^{2+} was so sensitive compared to that of $\mathbf{HL^1}$ that the concentration of examined $\mathbf{HL^2}$ was diminished as 10 μM with the $[Zn^{2+}]$ ranging from 0-20 equiv. in ethanol. Unlike that of $\mathbf{HL^1}$ with an ethoxyl group, addition of $ZnCl_2$ into $\mathbf{HL^2}$ in ethanol only induced enhancement of ligand-centered luminescence at 453 nm without any shift of emission peak and reached saturation when the ratio amounted to 1:1(Figure **8**). The UV absorption of $\mathbf{HL^2}$ also responds to titration of Zn^{2+} with a new absorption peak at 373 nm while that at 258, 319 nm decreased with four isosbetic points at 248, 269, 338, 291 nm (Figure **S8**). The binding ratio between Zn^{2+} and $\mathbf{HL^2}$ was determined to be 1:1 which was further confirmed by both job plot (Figure **S9**) and crystal structure (figure 10). More sensitivity of $\mathbf{HL^2}$ on Zn^{2+} could be supported by the relatively low limit of detection as 7×10^{-8} M ranging (Figure **S10**, LOD=3σ/slope, R^2=0.997) with a linearity range between 1×10^{-6} M and 9×10^{-6} M.

Likewise, selectivity of $\mathbf{HL^2}$ towards Zn^{2+} was examined by fluorescence of $\mathbf{HL^2}$ (Figure **9**) in the presence of equivmolar metal ions including Mn^{2+}, Fe^{2+}, Co^{2+}, Ni^{2+}, Cu^{2+}, Zn^{2+}, Na^+, K^+, Mg^{2+}, Ca^{2+}, Al^{3+}, Cr^{3+}, Hg^{2+}, and Fe^{3+} as their Cl^- salts (Hg^{2+} as

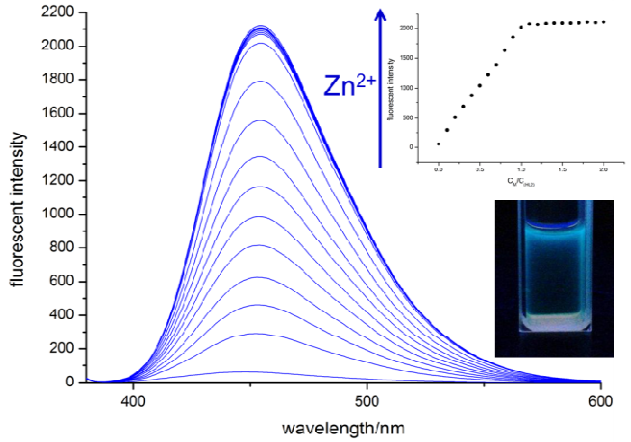

Figure 8. Fluorescence emission spectra of **HL²** upon addition of $ZnCl_2$ in ethanol. λ_{ex} = 350 nm at room temperature ([**HL²**] = 10μM; [Zn^{2+}] =0, 1.0, 2.0, 3.0, 4.0 5.0, 6.0, 7.0, 8.0, 9.0, 10.0, 11.0, 12.0 13.0, 14.0, 15.0, 16.0, 17.0, 18.0, 19.0, 20.0 μM .

its NO_3^- salt). The results revealed that Mn^{2+}, Fe^{2+}, Co^{2+}, Ni^{2+}, Cu^{2+}, Hg^{2+}caused slight quenching of fluorescence of **HL²** while Cd^{2+}, Na^+, K^+, Mg^{2+}, Ca^{2+}, Al^{3+}, Cr^{3+}, and Fe^{3+} induced slight fluorescence enhancement, indicating that **HL²** has high selectivity towards Zn^{2+}. Specifically, the selectivity of **HL²** on Zn^{2+} over Cd^{2+} was calculated as 30 using ratio of I_{Zn}/I_{Cd}, much

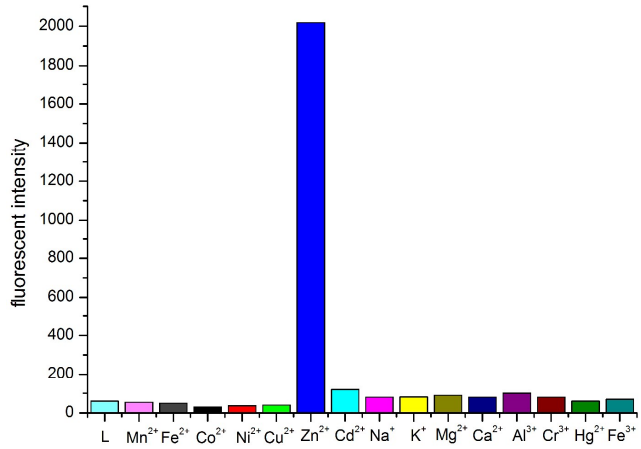

Figure 9. Fluorescence emission spectra of **HL²** in the presence of different ions such as Mn^{2+}, Fe^{2+}, Co^{2+}, Ni^{2+}, Cu^{2+}, Zn^{2+}, Cd^{2+}, Na^+, K^+, Mg^{2+}, Ca^{2+}, Al^{3+}, Cr^{3+}, Hg^{2+}, and Fe^{3+} (metal ions as their Cl^- salts and Hg^{2+} as NO_3^- salts) in ethanol. λ_{ex} = 330 nm, [**HL²**] = 10 μM, and [M^{n+}] =10 μM.

higher than that of **HL¹**. Furthermore, selectivity of **HL²** on Zn^{2+} was studied by fluorescence respond of Zn^{2+} in the presence of other competing metal ions including Mn^{2+}, Fe^{2+}, Co^{2+}, Ni^{2+}, Cu^{2+}, Zn^{2+}, Cd^{2+}, Na^+, K^+, Mg^{2+}, Ca^{2+}, Al^{3+}, Cr^{3+}, Hg^{2+}, and Fe^{3+}, results of which revealed that these metal ions have negligible disturbance on Zn-**HL²** fluorescence, further indicating high selectivity of **HL²** over Zn^{2+}(Figure **10**).

Crystal structure of $(ZnL^2Cl)_2$ (3) and $[Cd_4L^2{}_6]\cdot[CdCl_4]\cdot CH_3OH$ (4) and proposed mechanism for Zn^{2+} sensing of HL^1

Single crystal analysis revealed that compound **3** crystallized in monoclinic $P2_1/n$ space group and showed a centrosymmertric binuclear structure composed of two Zn^{2+} ions, two deprotonated $(L^2)^-$ anions and two chlorides. In this discrete unit, each Zn1 was penta-coordinated to two nitrogen atoms (N1, N2), one hydroxyl

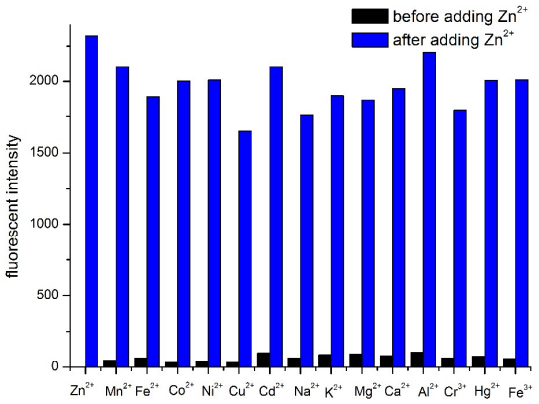

Figure 10. Selectivity of **HL²** for Zn^{2+} in the presence of other metal ions in ethanol. λ_{ex} = 350 nm. Black bars represent the addition of an excess of the appropriate metal ion (50μM for Na^+, K^+, Ca^{2+},Mg^{2+}, Fe^{3+}, Cu^{2+} and 30 μM for all other metal ions) to a 10 μM solution of **HL²**. Blue bars represent the subsequent addition of 0.1 mM $ZnCl_2$ to the solution.

oxygen atom (O1) from one ligand, one hydroxyl oxygen atom (O1a) from the other ligand and one chloride (Cl1) (Figure **11**). Upon coordination, N2O donor set of **L²** strongly chelated to Zn^{2+} and two hydroxyl oxygen atoms adopted μ_2-coordination modes to bridge two Zn^{II} ions together and formed the dinuclear structure.

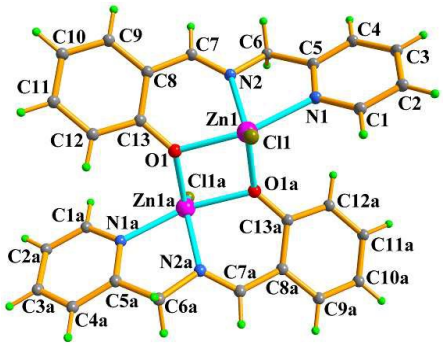

Figure 11. Molecular structure of dinuclear compound $[Zn(L^2)Cl]_2$ (**3**) with atomic labels. Asymmetry code: a)1-x,-y,-z.

Replacing $ZnCl_2$ with $CdCl_2$, **HL²** was deprotonated and coordinated to generate compound $\{[Cd_4L^2{}_6]\cdot[CdCl_4]\cdot CH_3OH\}_2\cdot H_2O$ (**4**) at room temperature. The single crystal analysis revealed that compound **4** crystallized in monoclinic $P2/c$ space group and possessed two anionic mononuclear $[CdCl_4]^{2-}$ units, two lattice methanol molecules, one water molecule and two independent tetranuclear cationic $[Cd_4L^2{}_6]^{2+}$ units associated with intermolecular hydrogen bonds C-H···Cl. It could be seen from Figure **12** that two tetranuclear $[Cd_4L^2{}_6]^{2+}$ cationic moieties containing one mirror symmetry are structurally identical, each comprising of four Cd^{2+} ions and six deprotonated ligand $(L^2)^-$. Four Cd^{2+} ions in each unit are hexa-coordinated to donor set N4O2 from two adjacent ligand $(L^2)^-$ for three cadmium ions (Cd2, Cd3, Cd3a/Cd5, Cd6, Cd6a) at the vertices of an equilateral triangle or donor set O6 from six ligand $(L^2)^-$ for one central cadmium ion (Cd1/Cd4), presenting the distorted octahedral coordination geometry. While each mononuclear anion unit contained one Cd^{2+} ion and four coordinated chlorides, presenting one tetrahedral coordination geometry. Together with lattice methanol and water molecules, cationic $[Cd_4L^2{}_6]^{2+}$ and anionic $[CdCl_4]^{2-}$ moieties were further connected each other by hydrogen bonds C-H···Cl(O) into the 2-D supramolecular layer (Figure **S11**).

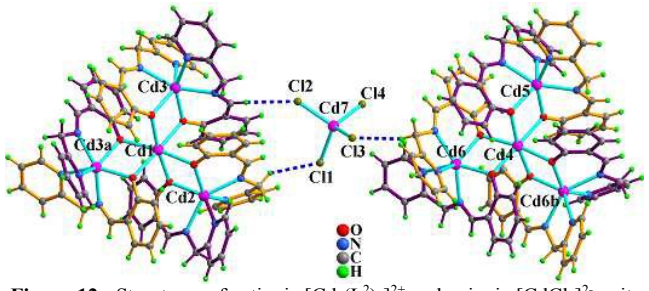

Figure 12. Structures of cationic $[Cd_4(L^2)_6]^{2+}$ and anionic $[CdCl_4]^{2-}$ units in compound **4** with partial atomic labels, and hydrogen atoms, the lattice water and methanol molecules are omitted for clarify. Symmetric code: a):1-x,y,1.5-z, b):-x,y,1.5-z

Luminescence spectrum of compound **3** in ethanol was also obtained to attest that the product upon titration of Zn^{2+} into $\mathbf{HL^2}$ is compound **3**.(Figure S) Similar to $\mathbf{HL^1}$, Zn-induced fluorescent intensity enhancement of ligand $\mathbf{HL^2}$ could be explained by CHFF, PET, and C=N isomerization-related process as mentioned above. Even though upon reaction of $\mathbf{HL^2}$ and $CdCl_2$, crystal of compound **4** can be obtained, yet instant fluorescent response cannot be detected upon titration of Cd^{2+} salts (anion as Cl^-, NO_3^-, ClO_4^-, or OAc^-) into $\mathbf{HL^2}$. This negative response could be possibly attributed to larger radius and therefore less affinity to $\mathbf{HL^2}$ of Cd^{2+} compared to that of Zn^{2+}, which could be supported by the difference of Cd-N, Cd-O distances and Zn-N, Zn-O distances in compound **3** and **4** (Table 1).[19] On the other hand, despite several reports of coordination compounds based on HL^2 and other metals[20] such as Fe(III),V(III), Cu(II), and Ni(II), yet high fluorescent sensing selectivity of $\mathbf{HL^2}$ towards Zn^{2+} can be also rationalized ascribing to paramagnetism of other metals which causes fluorescence quenching.

Table 1. Information of $\mathbf{HL^1}$ and $\mathbf{HL^2}$ as fluorescent sensors for Zn^{2+} and/or Cd^{2+}.

sensor	metal	binding ratio (M^{2+}: L)	Limit of detection	I_{Zn} / I_{Cd} (1 equiv.)	mean of metal–N distances (Å)	mean of metal-O distances(Å)	sensing mechanism
$\mathbf{HL^1}$	Zn^{2+}	4:3	1.1×10^{-6}M	4.8	2.098	2.020	TITC[1c], CHEF,PET[9] C=N isomerization[9,18]
	Cd^{2+}	2:1	9.2×10^{-6}M		2.315	2.302	CHEF, PET, C=N isomerization
$\mathbf{HL^2}$	Zn^{2+}	1:1	4.7×10^{-8}M	30	2.070	2.108	CHEF, PET, C=N isomerization
	Cd^{2+}	2:3	/		2.357	2.289	/

Conclusions

Ligands ($\mathbf{HL^1}$, $\mathbf{HL^2}$) as fluorescent sensors towards Zn^{2+} and/or Cd^{2+} and their metal ions sensing properties were investigated, through which we demonstrated the effect of ethoxyl substituent on Zn^{2+} fluorescent sensing. Their spectral difference in sensing Zn^{2+} or Cd^{2+} could be attributed to ethoxyl group which facilitated Zn^{II}-induced twisted intramolecular charge transfer. Such results may give insight into how to develop fluorescent sensors for discriminating ion pairs.

For $\mathbf{HL^1}$ with an ethoxyl substituent on the benzene ring, interaction of the ligand with Zn^{2+} induced twisted molecular structure and causes fluorescent red shift and fluorescent enhancement, while interaction of Cd^{2+} with $\mathbf{HL^1}$ merely induced fluorescence enhancement retaining the original emission peak. Though $\mathbf{HL^1}$ spectrally responds to both Zn^{2+} and Cd^{2+}, these two metal ions can be discriminated by $\mathbf{HL^1}$ via two coordination conformations.

For $\mathbf{HL^2}$ absent of the ethoxyl group, it has exclusive response towards Zn^{2+} over other metal ions including Cd^{2+}, showing that $\mathbf{HL^2}$ could also be a selective fluorescent sensor for Zn^{2+}. Unlike $\mathbf{HL^1}$, no spectral shift was detected upon interaction of $\mathbf{HL^2}$ with Zn^{2+}, which could be ascribed to absence of twisted molecular structure in Zn-$\mathbf{HL^2}$ compound **3**. Negative response of $\mathbf{HL^2}$ towards Cd^{2+} correlates with longer Cd-N, Cd-O bond distances compared with that of Zn-N, Zn-O bond lengths in compounds **3** and **4**, indicating less affinity of Cd^{2+} towards $\mathbf{HL^2}$. On the other hand, without ethoxyl group as hindrance effect, $\mathbf{HL^2}$ shows greater sensitivity towards sensing Zn^{2+} with a much lower detection limit for Zn^{2+}.

Acknowledgements

This work has been supported by the National Natural Science Foundation of China (Grant No.91122008, 21071056 and 21471061), Research Fund for the Doctoral Program of Higher Education of China (20124407110007), Guangdong Province of higher school science and technology innovation key project (cxzd1113), and Foundation for High-level Talents in Higher Education of Guangdong, China (C10301). The authors also thank Prof. Keith Man-chung Wong for offering valuable suggestions during composition of this essay.

Notes and references

(1) (a) P.J. Jiang, Z.J. Guo, *Coord. Chem. Rev.*2004, **248**, 205-229. (b) L. M. Wysockia, L. D. Lavis, *Curr. Opin. Chem. Biol.*, 2011, **15**, 752-759.(c) A. P. de Silva, H. Q. N. Gunaratne, T. Gunnlaugsson, A. J. M. Huxley, C. P. McCoy, J. T. Rademacher, T. E. Rice, *Chem. Rev.* 1997, **97**, 1515-1566.(d) K. P. Carter, A. M. Young, A. E. Palmer, *Chem. Rev.* 2014**, 114**, 4564−4601.(e*)* X. Li, X. Gao, W. Shi, H. Ma, *Chem. Rev.*, 2014, **114**, 590–659. (f) Y. B. Ding, T. Li, X. Li, W. H. Zhua, Y. S. Xie. *Org. Biomol. Chem.*, 2013, **11**, 2685; (g) Y. B. Ding, Y. S. Xie, X. Li, Jonathan P. Hill, W. B. Zhang, W. H. Zhu. *Chem. Commun.*, 2011, 47, 5431; (h) Y.B. Ding, X. Li, T. Li, W. H. Zhu, and Y.S. Xie, *J. Org. Chem*., 2013, **78**, 5328; (i) Y. B. Ding, Y. Y. Tang, W.H. Zhu, Y.S .Xie. *Chem. Soc. Rev.*, 2015,**44**, 1101-1112;

(2) (a) R. H. Holm, P. Kennepohl, E. I. Solomon, *Chem. Rev*.1996, **96**, 2239-2314. (b) D. S. Auld, *BioMetals*. 2001, **14**, 271-313. (c) A. I. Bush, *Trends Neurosci.* 2003, **26**, 207–214.(d) C. J. Frederickson, J. Y. Koh, A. I. Bush, *Nat. Rev. Neurosci.* 2005, **6**, 449–462. (e) A. B. Chausmer, *J. Am. Coll. Nutr.* 1998, **17**, 109–115.(f) E. L. Que, D. W. Domaille, C. J. Chang, *Chem. Rev.* 2008, **108**,1517−1549.

(3) (a) A. Voegelin, S. Poster, A. C. Scheinost, M. A. Marcus, R. Kretzsch mar, *Environ. Sci. Technol*., 2005, **39**, 6616-6623; (b) C. Rensing, R. M. Maier, *Ecotoxicol. Environ. Saf*., 2003, **56**, 140-147.

(4) (a) E. L. Que, D. W. Domaille, C. J. Chang, *Chem. Rev.* 2008, **108**, 1517−1549.(b) H. Woo, S. Cho , Y. Han, W.S. Chae, D.R. Ahn,

Y. You, W. Nam, *J. Am. Chem. Soc.*, 2013, **135** , 4771-4787 (c) X.A. Zhang, D. Hayes, S. J. Smith, S. Friedle, S. J. Lippard, *J. Am. Chem. Soc.* 2008, **130**, 15788−15789. (d) K. Hanaoka, K. Kikuchi, H. Kojima, Y. Urano, T. Nagano, *J. Am. Chem. Soc.* 2004**, 126**, 12470−12476.(e) K. Komatsu, K. Kikuchi, H. Kojima, Y. Urano, T. Nagano, *J. Am. Chem. Soc.* 2005**, 127**, 10197−10204. (f) K. Komatsu, Y. Urano, H. Kojima, T. Nagano, *J. Am. Chem. Soc.* 2007, **129**, 13447−13454.(g) H. Z. Su, X. B. Chen, W. H. Fang, *Anal. Chem.* 2014, **86**, 891−899 (h) Y. Mikata, K. Kawata, S. Iwatsuki, H. Konno, *Inorg. Chem.* 2012, **51**, 1859−1865. (i) J. T. Simmons, J. R. Allen, D. R. Morris, R. J. Clark, C. W. Levenson, M. W. Davidson, L. Zhu, *Inorg. Chem*. 2013, **52**, 5838−5850 (j) E. Kimura, S. Aoki, E. Kikuta, T. Koike, *Proc. Natl. Acad. Sci.* USA 2003, **100**, 3731–3736

(5) (a) Z. R. Grabowski, K. Rotkiewicz, *Chem. Rev.* 2003, **103**,3899-4031.(b) B. Valeur, I. Leray, *Coord. Chem. Rev*. 2000, **205**, 3-40

(6) (a) S. Aoki, D. Kagata, M. Shiro, K. Takeda, E. Kimura, *J. Am. Chem. Soc.* 2004, **126**, 13377–13390 (b) P. Mahato, S. Saha, A. Das, *J. Phys. Chem. C*, 2012, **116**, 17448–17457.

(7) (a) X.Y. Zhou, P.X. Li, Z. H. Shi, X. L. Tang, C. Y. Chen, W.-S. Liu. *Inorg. Chem.* 2012, **51**, 9226−9231.(b) E. M. Nolan, J. W. Ryu, J. Jaworski, R. P. Feazell, M. Sheng, S. J. Lippard, *J. Am. Chem. Soc.* 2006, **128**, 15517-15528.(c) F. A. Cotton and G. Wilkinson, *Advances in Inorganic Chemistry*, Wiley, New York, 5th edn, 1988, pp. 957–1358. (d) M. M. Henary, Y. G. Wu, C. J. Fahrni, *Chem.-Eur. J.* 2004, **10**, 3015.(e) R. D. Hancock, *Chem. Soc. Rev.*, 2013**, 42**, 1500-1524.

(8) (a) M. P. Waalkes, *Mutat. Res.* 2003, **533**, 107-120. (b) M. Waisberg, P. Joseph, B. Hale, D. Beyersmann, *Toxicology* 2003, **192**, 95-117. (b) M. P. Waalkes, T. P. Coogan, R. A. Barter, *Crit. Rev. Toxicol.* 1992, **22**, 175–201.

(9) V. Kumar, A. Kumar, U. Diwan, K. K. Upadhyay, *Dalton Trans*., 2013, **42**, 13078–13083

(10) Sheldrick, G. M. SADABS, version 2.05; University of Göttingen: Göttingen, Germany, 1996.

(11) G. M. Sheldrick, SHELXS-97, Program for X-ray Crystal Structure Determination; University of Göttingen: Göttingen, Germany, 1997.

(12) G. M. Sheldrick, SHELXS-97, Program for X-ray Crystal Structure Refinement, University of Göttingen: Göttingen, Germany, 1997.

(13) Z.P. Zheng, Y.J. Ou. X. J. Hong, L. M. Wei, L. T. Wan, W.H. Zhou, Q. G. Zhan, Y. P. Cai, *Inorg. Chem.* 2014, **53**, 9625−9632

(14) F. Robert, P. L. Jacquemin, B. Tinant, Y. Garcia, *CrystEngComm,* 2012, **14**, 4396 – 4406

(15) B. Bosnich, *J. Am. Chem. Soc*., 1968, **90** , 627–632

(16) (a)X. B. Li, M. Bera, G. T. Musiea, D. R. Powell, *Inorg. Chim. Acta.* 2008, ***36***, 1965–1972. (b) D. M. Cooper, G. Ronald, S. Hargreaves, P. Kennewell, J. Redpath, *Tetrahedron* 1995, **51**, 7791-7808, 1995

(17) G. f. Li, Magana, D. R. B. Dyer, *J. Phys. Chem. B*, 2012, **116**, 12590–12596

(18) (a) J. S. Wu, W.M. Liu, X. Q. Zhuang, F. Wang, P. F. Wang, S. L. Tao, X. H. Zhang, S.-K. Wu, S.T. Lee, *Org. Lett.* 2007, **9**, 33-36.(b) H. Jung, K. Ko, J. Lee, S. Kim, S. Bhuniya, J. Lee, Y. Kim, S. Kim, *Inorg. Chem.* 2010, **49**, 8552–8557. (c) S. Iyoshi, M. Taki, Y. Yamamoto, *Inorg. Chem.* 2008, **47**, 3946-3948.

(19) (a) N. J. Williams, W. Gan, J. H. Reibenspies, R. D. Hancock, *Inorg. Chem.* 2009**, 48**, 1407−1415.(b) Y. Mikata, Y. Sato, S. Takeuchi, Y. Kuroda, H. Konnoc, S. Iwatsuki, *Dalton Trans.*, 2013, **42**, 9688-9698.

(20) (a) C. Imbert, H. P. Hratchian, M. Lanznaster, M. J. Heeg, L. M. Hryhorczuk, B. R. McGarvey, H. B. Schlegel, C. N. Verani,. *Inorg. Chem.* 2005, **44**, 7414-7422. (b) S. P. Rath, K. K. Rajak, Chakravorty, *Inorg. Chem.*, 1999, **38**, 4376;(c) B. de Souza,; A. J. Bortoluzzi,; T. Bortolotto, F. L. Fischer, H. Terenzi, D. E. C. Ferreira, W. R. Rocha, A. Neves, *Dalton Trans.*, 2010, **39**, 2027.

Two Schiff base ligands for distiguishing Zn^{II}/Cd^{II} sensing-effect of substituent on fluorescent sensing

Zhi-Peng Zheng, Qin Wei, Wen-Xia Yin, Lin-Tao Wan, Xia Huang, Ying Yu*, Yue-Peng Cai*

Two Schiff base ligands (HL^1, HL^2) were facially synthesized as fluorescent sensors for distinguishing sensing of Zn^{2+}or Cd^{2+}, in which the substituent ethoxyl group plays an important role in metal ions sensing property. With an ethoxyl group, HL^1 presents fluorescence spectral red shift and intensity enhancement, while shows merely intensity enhancement upon titration of Cd^{2+}. Absent of the ethoxyl group, HL^2 exclusively responds to Zn^{2+} with only fluorescence intensity enhancement.